A Study of Channel Model Parameters for Aerial Base Stations at 2.4 GHz in Different Environments

Navuday Sharma[1], Maurizio Magarini[1], Laura Dossi[2], Luca Reggiani[1], Roberto Nebuloni[2]
[1]Politecnico di Milano,Italy.
[2]IEIIT, Consiglio Nazionale delle Ricerche (CNR), Milan, Italy.
Email: {navuday.sharma,maurizio.magarini,luca.reggiani}@polimi.it,{laura.dossi,roberto.nebuloni}@ieiit.cnr.it

***Abstract*—The 5^{th} generation of cellular networks (5G) will provide high speed and high-availability wireless links for communication between mobile users. The usage of aerial platforms as base stations has been recently proposed to meet the above requirements, especially in densely-packed urban areas. To make an accurate prediction of the performance in such a communication system the availability of suitable channel models is a fundamental requirement. Here, we concentrate on a simple path loss and shadow fading channel model that is commonly used to describe the propagation between an aerial base station and a user on the ground. A commercial 3D ray-tracing simulator is used to extract the main parameters used in the model and the Line of Sight/Non Line of Sight probabilities as a function of the transmitter height and elevation angle. We consider three reference scenarios: Suburban, Urban and Urban High Rise generated according to ITU-R specifications. As a novel contribution, we also show simulation results for the spatial correlation of the received signal in the three considered scenarios.**

***Index Terms*—Path loss model, radio propagation, shadow fading, aerial base stations, ray-tracing simulation, air-to-ground communication, unmanned aerial vehicles.**

I. Introduction

In the past decade, the growth and development of wireless technology has led to the quick adoption of smart devices such as phones, tablets, watches, and wearables for health monitoring, with machine type communication. For such devices there are different requirements like high data rate, high reliability, and low latency. These requirements will be fulfilled by 5G for which the possible scenarios and the envisioned applications are illustrated in [1], [2]. Recently, several research works have considered the possibility of satisfying these requirements by installing cellular base stations on aerial platforms [3], [4]. As is well known, Unmanned Aerial Vehicles (UAVs) are currently used both in military and commercial industry for many different applications like search and rescue, surveillance and reconnaissance, weather detection, 3D mapping, monitoring wildlife, farming etc [5].

The use of UAVs with an onboard base station has been considered in several papers [6]–[8]. One of the main advantages of having base station onboard a UAV is that of dynamically changing the coverage area according to traffic intensity. Moreover, the use of a UAV as flying base stations allows to provide better cellular coverage and boosting the capacity of the mobile user stations at ground [9], [10]. Such a system is cost effective and it is also highly efficient in situations where a large mass of users confined in a small area demand high speed data as in stadiums, public rallies, festivals, concerts etc. In these situations, UAVs can fly near to the crowd for fulfilling data requirements [7]. However, a safe flying distance for such an operation has not been standardized yet.

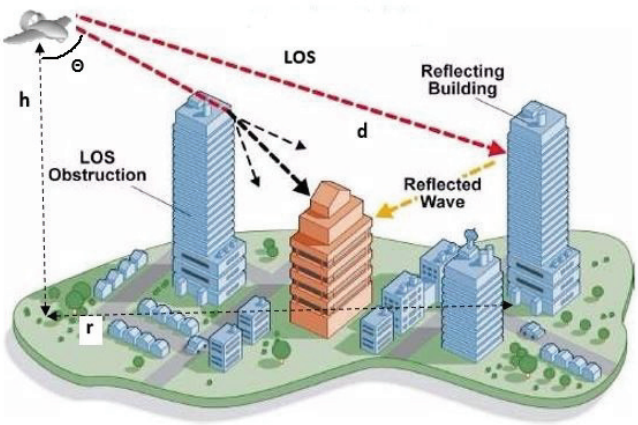

Fig. 1. Example of LoS and NLoS links.

Both low (LAPs) and high altitude aerial platforms (HAPs) have been considered for proximity applications [11]. While either a UAV or an airship can be used to implement an HAP, only a UAV seems to be a promising platform for LAPs. This limitation is due to the large size of the airship, its low payload capacity, low speed, and difficult maneuverability that prevents it to fly at altitudes near to the mobile users on the ground. However, small UAVs such as quadcopters are easier to deploy and can fly close to the ground, thus providing better services to the users with a line of sight (LoS). Therefore, we have chosen LAPs/UAVs for our simulations since they provide better flexibility for small cells.

The growing interest for such aerial base stations demands for the development of channel models that allows predicting fundamental quantities such as the average propagation Path Loss (PL) and the standard deviation of the Shadow Fading (SF). Models for PL and SF have been proposed in [12] for LAPs and in [13] for HAPs, respectively, as a function of the transmitter-to-receiver elevation angle. The elevation angle includes the PL dependence on both the transmitter-to-receiver

978-1-5386-4790-5/18/$31.00 ©2018 IEEE

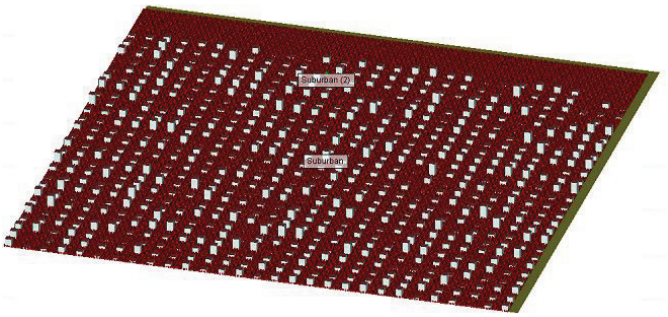

(a) Suburban Scenario

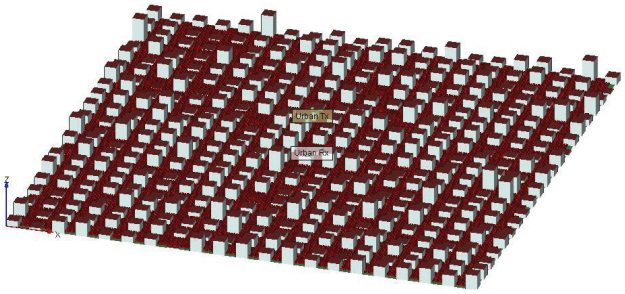

(b) Urban Scenario

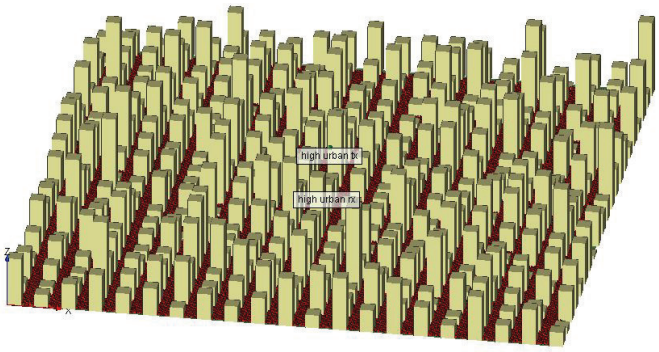

(c) Urban High Rise Scenario

Fig. 2. Measurement environments used for ray tracing simulations.

horizontal distance and the transmitter height. However, our study is constrained to LAPs only and, therefore, a different approach is adopted here. First, the Close-in (CI) propagation model, *i.e.*, a standard approach for path-loss prediction that uses a $d_0 = 1\,\text{m}$ close-in free space reference distance, is considered [14]. The CI model depends on two parameters that are the Path Loss Exponent (PLE) and the standard deviation of large scale shadowing σ. Both the two parameters are calculated as a function of the transmitter height and link elevation angle. This procedure highlights the effects of the transmitter height and elevation angle, being the fundamental design parameters. Moreover, we distinguish between LoS and non-LoS (NLoS) cases according to the presence or absence of the free-space LoS path in the simulated link, whereas in [12] they are estimated from the shape of the PL histogram across the test area. This allows to calculate the corresponding PLEs

TABLE I
CITY LAYOUT PARAMETERS

Scenario	α_0	β_0	γ_0	Number of Buildings	Building Width (m)	Street Width (m)
Suburban	0.1	750	8	750	11.54	24.97
Urban	0.3	500	15	500	24.49	20.23
Urban High Rise	0.5	300	50	300	40.82	16.91

TABLE II
MATERIAL PROPERTIES USED IN SIMULATION

Material	Thickness (m)	Roughness (m)	Conductivity	Permittivity
Concrete	0.3	0	0.05	6
Wet earth	0	0	0.02	25

together with their associated LoS probabilities as a function of the transmitter height. Therefore, we improve the prediction of PLE and standard deviation of SF for LoS and NLoS bringing novelty to our work. We follow a probabilistic approach, which is not addressed in the previous works. These are useful parameters for air to ground channel (A2G) which are modeled with Rician fading in different environments, created for simulation, as described in Section II. Also, we investigate spatial correlation of shadowing in these three considered scenarios, which has not been addressed in previous works.

The paper is organized as follows. Section II describes the measurement scenarios created for ray tracing simulation. Section III shows the Path Loss model. Section IV reports the simulation results. Finally, Section V draws the conclusions.

II. MEASUREMENT SCENARIOS

For developing the model, 3D ray tracing simulations were performed using Wireless InSite simulator 3.0.1 [15], which is an accurate calculation tool for designing mobile wireless systems [16]. Three simulation environments were created in 3DS MAX [17] for Suburban, Urban and Urban High Rise scenarios, as shown in Fig. 2, with maximum building heights and density in Urban High Rise, lower in Urban and minimum in Suburban scenario. The three scenarios were created based on the parameters α_0, the fraction of land area covered by buildings, β_0, the mean number of buildings per unit area, and γ_0, a parameter related to building height distribution, as given by ITU-R document [12]. The simulation area was chosen equal to $2000 \times 2000\,\text{m}^2$ to reduce the computation time while maintaining the accuracy to snapshots of size $1000 \times 1000\,\text{m}^2$ selected from the larger area. Two snapshots from each scenario were simulated to improve the accuracy of numerical results. Building width and street width were calculated following [12] using the parameters shown in Table I. The terrain is assumed to be flat. The properties of the materials used for the terrain and the external walls and the rooftops of the buildings are described in Table II. We have used concrete for the buildings and wet earth for the terrain. In Fig. 2, the red dots patched on the streets are the receiving mobile users. The transmitter, *i.e.*, the aerial base station, is in

the center of the area at a certain height. A number of approximately $32,500$ receivers spaced $5\,\text{m}$ apart in each direction from each other was used for simulation. All receivers were $2\,\text{m}$ above the ground and equipped with an isotropic antenna. The receiver threshold was kept $-120\,\text{dBm}$ and the noise figure was set to $3\,\text{dB}$, keeping in consideration the practical RSSI (Received Signal Strength Indicator) values for LTE supported cellphones. The simulations were repeated placing the transmitter at increasing heights from 100 to $2000\,\text{m}$, with step of $100\,\text{m}$, in order to appreciate the sensitivity of the results to the height of the transmitter. The antenna at the transmitter was assumed to be isotropic with a transmitting power of $18\,\text{dBm}$. The voltage standing wave ratio (VSWR), which defines the amount of power reflected from the antenna, was set to 1. Also, standard sea level atmospheric conditions were used to perform the simulations. A sinusoidal waveform was transmitted with frequency of $2.442\,\text{GHz}$ spanning a bandwidth of $20\,\text{MHz}$.

III. Path loss Model

A. Overview

In our study we have considered CI free space reference distance PL model as it is a standard approach for describing propagation at any frequency and it is more stable, simple, and reliable than other models such as, for example, ABG model [14], [18]. The model is based on two fundamental parameters, the Path Loss Exponent (PLE) and the standard deviation of fading σ, both dependent on the environment. Typical values of path loss exponent are $\text{PLE} = 2$, for free space propagation, and $\text{PLE} = 4$, for two ray propagation and asymptotically large link distance [19].

The large-scale shadowing PL equation is given by

$$PL(d)[\text{dB}] = 20\log_{10}\left(\frac{4\pi d_0}{\lambda}\right) + 10n\log_{10}(d) + X_\sigma, \quad (1)$$

where λ is the wavelength, n is the PLE, d is the link distance, $d_0 = 1\,\text{m}$, and X_σ, in dB, is the log-normal random variable with standard deviation σ. Considering that for A2G communication in Suburban, Urban and Urban High Rise environments, increasing the height of the transmit antenna and the link elevation, the propagation characteristics result are much more sensitive to LoS and NLoS conditions as seen in Section IV. To improve path loss prediction we decided to follow a LoS probabilistic approach, proposed in [20], which provides analytically and graphically, the relation between LoS probability and elevation angle for LAP, based on mathematical steps defined by ITU-R for modeling LoS probability. Hence, the CI model and the probabilistic approach for LoS and NLoS path losses can be combined as

$$PL_{LoS}(d)[\text{dB}] = 20\log_{10}(\frac{4\pi d_0}{\lambda}) + 10n_{LoS}\log_{10}(d) + X_{\sigma,LoS}, \quad (2)$$

$$PL_{NLoS}(d)[\text{dB}] = 20\log_{10}(\frac{4\pi d_0}{\lambda}) + 10n_{NLoS}\log_{10}(d) + X_{\sigma,NLoS}, \quad (3)$$

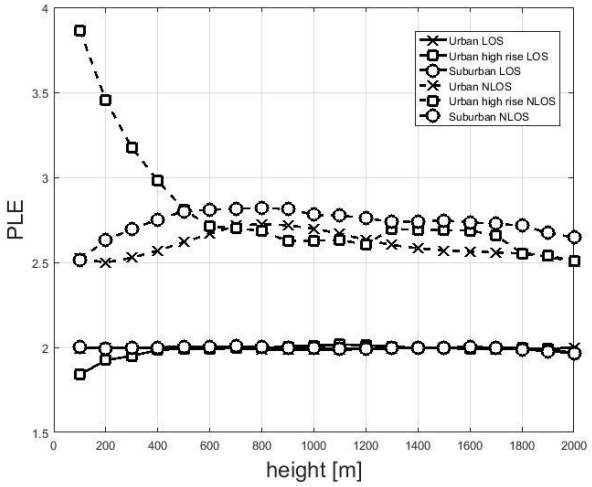

Fig. 3. PLE as a function of the transmitter height for LoS (continuous line) and NLoS (dashed line) in different environments.

$$PL(d)[\text{dB}] = P_{LoS}\cdot PL_{LoS}(d)[\text{dB}] + (1 - P_{LoS})\cdot PL_{NLoS}(d)[\text{dB}], \quad (4)$$

where P_{LoS} is the probability of having a LoS link, defined as a link where one of the paths is free space LoS, $PL_{LoS}(d)[\text{dB}]$ is the path loss when the link is in LoS condition, with parameters n_{LoS} and σ_{LoS}, and $PL_{NLoS}(d)[\text{dB}]$ is the path loss when the link is in NLoS condition, *i.e.*, there is no a free space LoS path, with parameters n_{NLoS} and σ_{NLoS}.

The values of the model parameters, P_{LoS}, n_{LoS} and σ_{LoS}, n_{NLoS} and σ_{NLoS} are studied separately as function of the height of the transmit antenna and of the elevation angle of the link (by taking also into account the 3D link distance d between transmitter and receiver and the transmitter height h). From the simulation results of the path loss we used the mathematical closed form expressions to derive the best model parameters by minimizing the standard deviation of the shadowing term, as given in [14]:

$$X_\sigma = PL(d)[\text{dB}] - 20\log_{10}(\frac{4\pi d_0}{\lambda}) - 10n\log_{10}(d) = A - nD, \quad (5)$$

where A represents $PL(d)[\text{dB}] - 20\log_{10}(\frac{4\pi d_0}{\lambda})$ and D represents $10\log_{10}(d)$. Then, the SF standard deviation is given as

$$\sigma = \sqrt{\frac{\sum X_\sigma^2}{N}} = \sqrt{\frac{\sum (A - nD)^2}{N}}, \quad (6)$$

where N is the number of simulated path loss points. Thus minimizing σ means minimizing $\frac{\sum (A-nD)^2}{N}$, *i.e.*, by setting to zero its derivative w.r.t. n in order to derive the PLE as

$$n = \frac{\sum DA}{\sum D^2}. \quad (7)$$

IV. Simulation Results and Analysis

The propagation links simulated by ray tracing software can be either LoS or NLoS, as shown in Fig. 1.

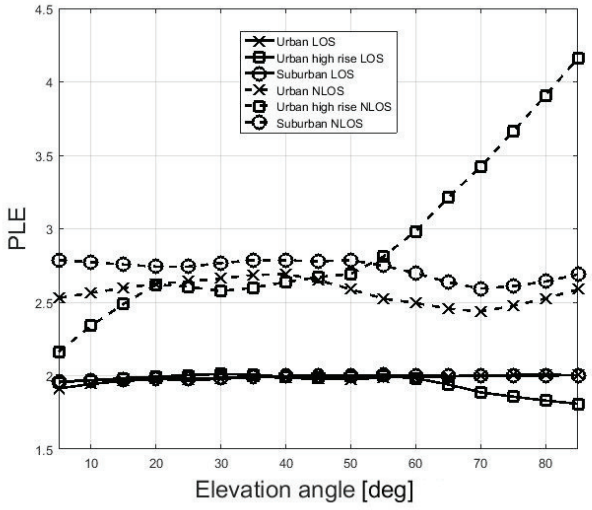

Fig. 4. PLE as a function of the link elevation for LoS (continuous line) and NLoS (dashed line) in different environments.

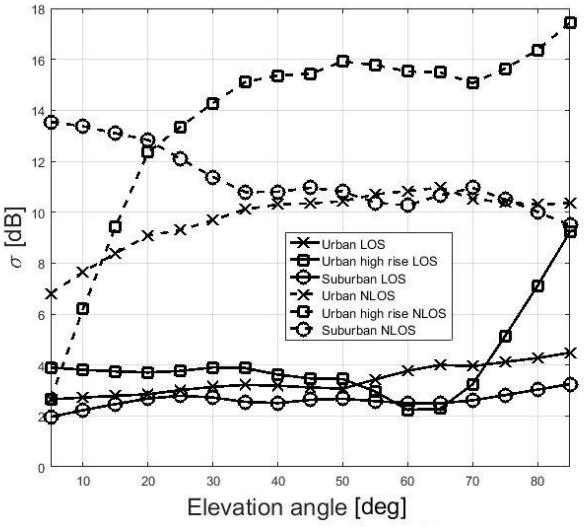

Fig. 5. Standard deviation of Shadowing as a function of elevation angle for LoS (continuous line) and NLoS (dashed line) links in different environments.

Figs. 3 and 4 shows the PLE against the transmitter height h and the elevation angle θ, respectively, for the three scenarios considered in the cases of LoS and NLoS links. The interpretations of the results as a function of the elevation angle are not straightforward. In fact, being $\cos\theta = \frac{h}{d}$, where d is the 3D link distance between transmitter and receiver, as seen in Fig. 1, same elevation angles correspond to different couples (h, d). For LoS links both the figures show PLE values around 2, as expected from propagation theory, since LoS path contribution is dominant. In the NLoS case, PLE values shown in Fig. 3 range between about 2.5 and 3 in Suburban and Urban environment but in Urban High Rise environment, instead, for heights less than $400m$, PLE increases due to strong reflections from nearby tall buildings. PLE patterns versus elevation (Fig. 4) in NLoS links are similar as the ones versus height for all the scenarios. This is due to the geometrical considerations, where elevation angle is higher when transmitter height is low, considering d to be constant for all the receivers as seen from the cosine relationship between h and d, previously. Therefore, also in Urban High Rise case, PLE exhibits an increasing trend for elevation angle $\theta > 60°$.

Concerning the random large-scale shadow fading, we derive from simulations, the theoretical amplitude as log-normal distributed of shadowing samples obtained from receivers radially moving away from the transmitter, for different transmitter heights in all simulated scenarios. Analogously to previous PLE curves, Figs. 5 and 6 show the standard deviation $\sigma[\mathrm{dB}]$ against the transmitter link elevation angle and the height, respectively, for the three scenarios considered in the cases of LoS and NLoS links. For LoS links, Fig. 6 highlights standard deviation values around 3 to 5 dB independently from the height. In the NLoS case, standard deviations vary between 10 to 17 dB and they increase with transmitter height, showing similar values in both LoS and NLoS links. Again, the standard

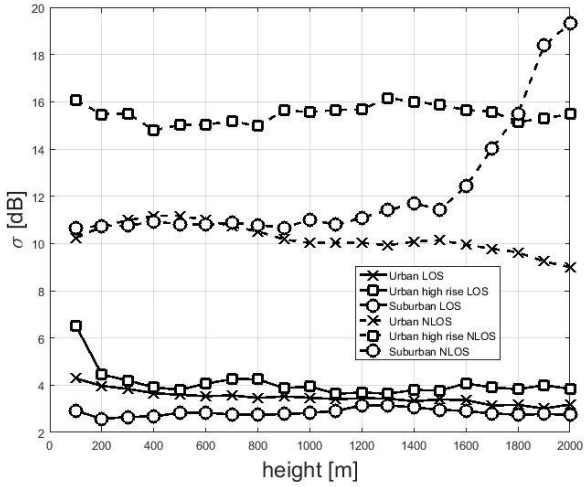

Fig. 6. Standard deviation of Shadowing as a function of transmitter height for LoS (continuous line) and NLoS (dashed line) links in different environments.

deviation values in Fig. 5 exhibit a clear trend for all scenarios. Standard deviation is higher for Urban High Rise scenario than Urban one because of the dense environment and tall buildings. In the LoS case w.r.t. the elevation angle, σ still remains approximately constant and, again, is clearly lower than in NLoS cases.

Figs. 8 and 9 show the Rice factor K, defined for LoS links as the ratio between the power in LoS path and the sum of power in NLoS paths, again as function of the transmitter height and elevation angle. The Urban High Rise case shows a clear increasing trend with the height while the Urban case shows a constant behavior and Suburban case shows a decreasing trend till $1200m$. This is due to a higher probability of LoS paths blockage in Urban High Rise and Urban

scenarios at low transmitter heights while the inverse is true for the Suburban one, due to low building density and heights. Therefore, we obtain Rician fading for Suburban scenarios and almost Rayleigh fading for Urban High Rise at low transmitter heights and Ricean fading at high transmitter heights for all the scenarios, as observed also in [21] for A2G channels. When we gather and average the results w.r.t. the elevation angle, as in Fig. 9, we see that at very high elevation angles (greater than $60°$), K in Urban High Rise scenarios decreases remarkably (this case corresponds to the low transmitter heights) because of the dense multipath reflections from buildings. It appears reasonable to assume, for all elevation angles, K between 1.5 and 2 for Suburban case, 1.5 for Urban one and, for Urban High Rise, 1 up to $60°$ and then decreasing till to 0 at $85°$.

Finally, Fig. 7 shows the spatial correlation of shadowing over the considered scenarios as in [14]. The correlation of each receiver with its neighboring receiver is calculated and plotted with respect to the distance of each receiver from transmitter. Receivers are present 5m apart from each other. The correlation was found to have a similar behavior along different directions due to the homogeneous nature of the environments. Therefore, in Fig. 7, we show correlation along one direction only. It was observed for the three scenarios that correlation is higher for the receivers near to the transmitter and decreases as the distance from transmitter increases. Also, correlation was found to be very low for low transmitter heights except in the case of Urban High Rise scenario where the transmitter is below the buildings heights and high correlation can be observed. It was observed that correlation increases from low transmitter heights to higher ones but after a certain threshold again start decreasing as seen for 1500m and 2000m transmitter heights. Also, a smooth behavior of the curves can be seen at higher transmitter heights with a higher correlation and anti-correlation values.

V. Conclusions

In this paper, the Close-in (CI) propagation model is applied to the simulated results obtained by a 3-D ray-tracing software on a random city scenario generated using ITU parameters, for LAP acting as a aerial base station for providing cellular coverage to ground users. The simple Close-in (CI) propagation model assumes the well-known dependence of the Path Loss (in dB) on the logarithm of the distance multiplied by the Path Loss Exponent (PLE).

In our study the PLE and the standard deviation of the shadowing is calculated as a function of the transmitter height and the elevation angle of the link, highlighting the effects of the transmitter height alone which is the fundamental design parameter. Moreover, LoS and NLoS cases are distinguished based on the presence or not of the free-space LoS path in the simulated link (whereas in [12] they were estimated from the shape of the PL histogram across the test area), and the corresponding PLE, Shadow Fading Standard deviation and Rice factor, are calculated again as a function of elevation angle and transmitter height, to better understand the role of global geometrical parameters in the different environment.

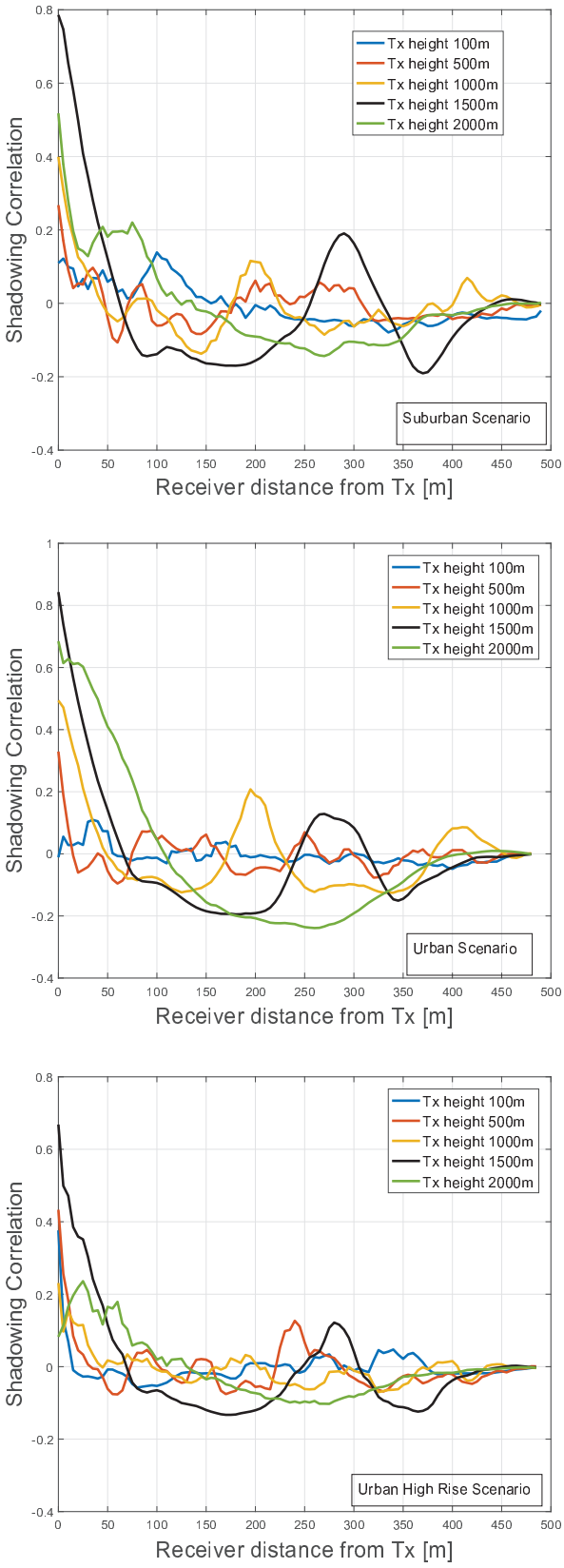

Fig. 7. Spatial Autocorrelation of Shadow fading over (a)Suburban (b)Urban and (c)Urban High Rise

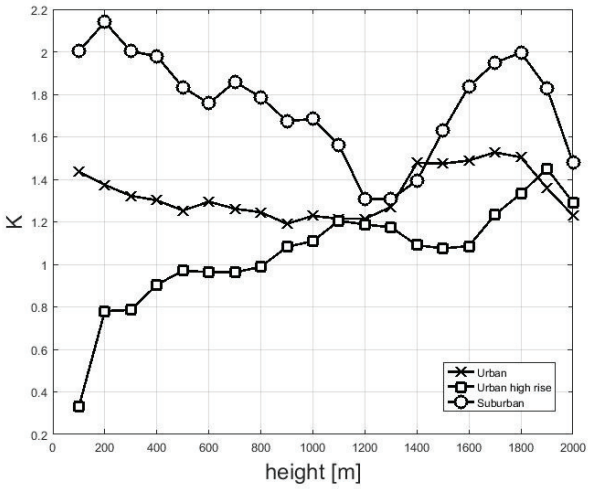

Fig. 8. Rice factor K as function of transmitter height in different environments.

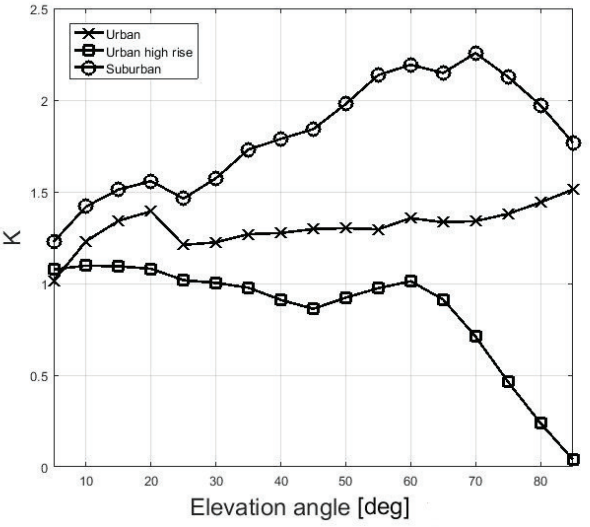

Fig. 9. Rice factor K as function of elevation angle in different environments.

Also, Spatial Correlation for Shadow fading was simulated for three considered environments and the behavior of the correlation with respect to the transmitter height and receiver distance from transmitter was shown.

REFERENCES

[1] A. Osseiran, F. Boccardi, V. Braun, K. Kusume, P. Marsch, M. Maternia, O. Queseth, M. Schellmann, H. Schotten, H. Taoka *et al.*, "Scenarios for 5g mobile and wireless communications: the vision of the metis project," *IEEE Communications Magazine*, vol. 52, no. 5, pp. 26–35, 2014.

[2] J. G. Andrews, S. Buzzi, W. Choi, S. V. Hanly, A. Lozano, A. C. Soong, and J. C. Zhang, "What will 5g be?" *IEEE Journal on Selected Areas in Communications*, vol. 32, no. 6, pp. 1065–1082, 2014.

[3] Cellular Drone Communication. https://www.qualcomm.com/invention/technologies/lte/advanced-pro/cellular-drone-communication.

[4] Connected UAVs. https://networks.nokia.com/products/ConnectedUAVs.

[5] S. Hayat, E. Yanmaz, and R. Muzaffar, "Survey on unmanned aerial vehicle networks for civil applications: A communications viewpoint," *IEEE Communications Surveys Tutorials*, vol. 18, no. 4, pp. 2624–2661, Fourthquarter 2016.

[6] I. Bor-Yaliniz and H. Yanikomeroglu, "The new frontier in ran heterogeneity: Multi-tier drone-cells," *IEEE Communications Magazine*, vol. 54, no. 11, pp. 48–55, November 2016.

[7] V. Sharma, M. Bennis, and R. Kumar, "Uav-assisted heterogeneous networks for capacity enhancement," *IEEE Communications Letters*, vol. 20, no. 6, pp. 1207–1210, June 2016.

[8] R. I. Bor-Yaliniz, A. El-Keyi, and H. Yanikomeroglu, "Efficient 3-d placement of an aerial base station in next generation cellular networks," in *Communications (ICC), 2016 IEEE International Conference on*. IEEE, 2016, pp. 1–5.

[9] M. Mozaffari, W. Saad, M. Bennis, and M. Debbah, "Efficient deployment of multiple unmanned aerial vehicles for optimal wireless coverage," *arXiv preprint arXiv:1606.01962*, 2016.

[10] ——, "Optimal transport theory for power-efficient deployment of unmanned aerial vehicles," in *Communications (ICC), 2016 IEEE International Conference on*. IEEE, 2016, pp. 1–6.

[11] M. Kong, O. Yorkinov, T. H. V. Tran, and S. Shimamoto, "Elevation angle-based diversity access employing high altitude platform station and unmanned aerial vehicle (uav) for urban area communications," 2011.

[12] A. Al-Hourani, S. Kandeepan, and A. Jamalipour, "Modeling air-to-ground path loss for low altitude platforms in urban environments," in *2014 IEEE Global Communications Conference*. IEEE, 2014, pp. 2898–2904.

[13] J. Holis and P. Pechac, "Elevation dependent shadowing model for mobile communications via high altitude platforms in built-up areas," *IEEE Transactions on Antennas and Propagation*, vol. 56, no. 4, pp. 1078–1084, 2008.

[14] S. Sun, T. S. Rappaport, S. Rangan, T. A. Thomas, A. Ghosh, I. Z. Kovacs, I. Rodriguez, O. Koymen, A. Partyka, and J. Jarvelainen, "Propagation path loss models for 5g urban micro-and macro-cellular scenarios," *arXiv preprint arXiv:1511.07311*, 2015.

[15] http://www.remcom.com/wireless-insite.

[16] P. Medeović, M. Veletić, and Ž. Blagojević, "Wireless insite software verification via analysis and comparison of simulation and measurement results," in *MIPRO, 2012 Proceedings of the 35th International Convention*. IEEE, 2012, pp. 776–781.

[17] https://www.autodesk.com/products/3ds-max/overview.

[18] T. A. Thomas, M. Rybakowski, S. Sun, T. S. Rappaport, H. Nguyen, I. Z. Kovacs, and I. Rodriguez, "A prediction study of path loss models from 2-73.5 ghz in an urban-macro environment," *arXiv preprint arXiv:1512.01585*, 2015.

[19] A. Goldsmith, *Wireless communications*. Cambridge university press, 2005.

[20] A. Al-Hourani, S. Kandeepan, and S. Lardner, "Optimal lap altitude for maximum coverage," *IEEE Wireless Communications Letters*, vol. 3, no. 6, pp. 569–572, Dec 2014.

[21] A. Zajić, *Mobile-to-mobile wireless channels*. Artech House, 2012.